Article

GA-Based Optimization for Multivariable Level Control System: A Case Study of Multi-Tank System

Ing Ming Chew[a,*], Filbert H. Juwono[b], and Wei Kitt Wong[c]

Department of Electrical and Computer Engineering, Faculty of Engineering and Science, Curtin University Malaysia, Sarawak, Malaysia
E-mail: [a,*]chewim@curtin.edu.my (Corresponding author), [b]filbert.hilman@curtin.edu.my, [c]weikitt.w@curtin.edu.my

Abstract. This paper presents a systematic way to determine the trade-off optimized controller tunings using computation optimization technique for both servo and regulatory controls of the Multi-Tank System, as one of the applications under the multivariable loop principle. The paper describes an improved way to obtain the best Proportional-Integral (PI) controller tunings in reducing the dependency on engineering knowledge, practical experiences and complex mathematical calculations. Relative Gain Array (RGA) calculation justified the degree of relation and the best pairing for both interacted control loops. Genetic Algorithm (GA), as one of the most prestigious techniques, was used to analyze the best controller tunings based on factor parameters of iterations, populations and mutation rates to the applied First Order plus Dead Time (FOPDT) models in the multivariable loop. Amid simulation analysis, GA analysis's reliability was justified by comparing its performance with the Particle Swarm Optimization (PSO) analysis. The research outcome was visualized by generating the process responses from the LOOP-PRO's multi-tank function, whereby the GA tunings' responses were compared with the conventional tuning methods. In conclusion, the result exhibits that the GA optimization analysis has successfully demonstrated the most satisfactory performance for both servo and regulatory controls.

Keywords: Multi-tank system, multivariable loop, relative gain array, genetic algorithm, control performance.

1. Introduction

One of the most common operated control loops in many industries is the Multi-Input-Multi-Output (MIMO) loop [1], also known as the multivariable loop. Recently, the multivariable loop has been applied to several engineering practices include heat pump system [1], quadruple-tank process [2], aero-engine [3], domestic boiler system [4], energy storage [5] and buildings climate control [6]. Furthermore, Multi-Tank System has also applied multivariable loop, whereby the system controls several process parameters concurrently in their respective loops with the independent set values [7]. However, controlling one of the loops will directly or indirectly affect the control capability of the other loops due to the interactions among the controlled loops. Controller tunings should be applied to maintain the high performance and stability of the control loops. Literature reflects that most of the industrial control loops apply PID controller [8], which consists of the Proportional-Integral (PI) and Proportional-Integral-Derivative (PID) control modes [9]. PID controller is chosen because is simple, cost-efficient, and effective in controlling the process, making it highly adaptable to various process conditions [10, 11]. The PID controller tunings can be manually done right in the first place to cope with the setpoint changes, imposed disturbances, or dynamic behavior changes after the modification has been made to the physical process. There are many tuning methods available for PID controllers, for instance, Ziegler-Nichols (ZN), Internal Model Control (IMC), which can be comprehended by most of the users in their applications [12]. To improve control performance, three control terms of proportional, integral and derivative gains are adopted to single, cascade and feedforward control loops [13, 14].

One typical example of a multivariable loop is the Two-Input-Two-Output (TITO) loop, as illustrated in Fig. 1. The interaction among the loops is known as cross-couplings. TITO loop has extended characteristics as compared to the single control loop, where TITO contemplates the interaction and control performance among two interacted processes [15]; in Fig. 1, U_1 interacts the effect of control action from the first loop to the second loop and U_2 interacts the effect of control action from the second loop to the first loop. Therefore, both manipulated U_1 and U_2 affect the output values Y_1 and Y_2. When the controller G_{C1} manipulates value, U_1, to keep Y_1 at setpoint SP_1, however, it will affect the performance of the output, Y_2. Then, controller G_{C2} responds to maintain output, Y_2 at setpoint SP_2, causing further interaction to the output, Y_1 and consequently affects the control action of the controller G_{C1}. The impact to both outputs consequence further changes to U_1 and U_2 due to the adjustment of controllers of both loops. For the reasonable controller tunings, the outputs might be stabilized after a certain period.
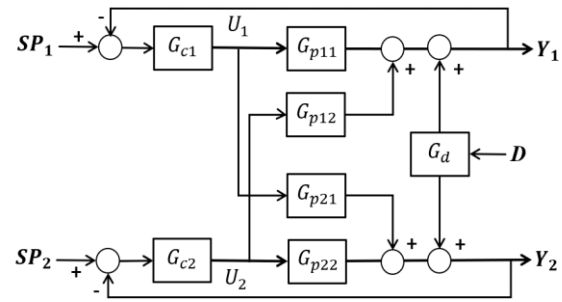

Fig. 1. Block diagram of TITO Loop.

The controller tuning task for the multivariable loop is challenging. The interaction among each loop may deteriorate the controllers' capability for both controlled loops [16]. As affected by other loops, the set controller tunings result in longer deadtime, more oscillatory responses, destabilizes the controlled loops and eventually result in the unforeseen loss of productivity in the process [17]. The authors in [18] stated that the manual detuned-PID controller settings could somehow minimize interaction between control loops, but the overall tunings strategy for multivariable loop still needs to be improved. In this sense, designing a highly efficient controller becomes extremely important in controlling the multivariable loop [1]. To date, the multivariable loop can be regulated by applying either the centralized or decentralized control scheme. The decentralized control scheme is more commonly applied via each loop's independent PID controller tunings. In addition, a decentralized control scheme applies a pairing factor among the interacted loops but still requires state-of-the-art refine tuning even after applying mathematical calculations to obtain the controller tunings. In a nutshell, it relies on the skills and end-user experiences, whereby only the experienced operators can reasonably obtain the controller settings for the satisfactory performance of the multivariable loop.

To minimize the dependency on personal skills and experiences during the controller tunings, computational optimization is a good alternative of choice to consider. Among many optimization approaches, Genetic Algorithm (GA) is selected for the analysis. GA performs analysis based on exploration and exploitation capabilities of natural evolution in solving optimization problems [19]. The primary stage cover selection, crossover, and mutation supported by the developed objective function. GA develops a number of chromosomes as population of potential solutions for calculating the best fitness function in the search region [20]. The objective function would interactively go through many generations and eventually obtain global solutions to the analyzed engineering problems. This paper aims to present a sound and direct way to analyze the trade-off controller setting using GA analysis for the best control performance of both servo and regulatory controls, replacing the present tuning practices that require the repetitive tunings for the respective servo or regulatory controls, which is yet to commit the overall

control performance. The GA analysis covers factors such as iterations, populations and mutation rate and later the result is compared to Particle Swarm Optimization (PSO) analysis. As the First Order plus Dead Time (FOPDT) models is applied in the multivariable loop, this research can be sound reference to the future GA optimization research for other multivariable based engineering applications, which is formed by FOPDT models. The paper is organized as follows:

Section 2 presents the literature study on multivariable control, PSO and GA. Section 3 depicts research methodology and development of block diagram for the LOOP-PRO software's multi-tank function, Routh-Hurwitz necessity analysis, Routh Gain Array (RGA), PSO and GA analysis. Section 4 presents GA analysis based on iteration, population and mutation rate criteria. Then, it incorporates other criteria to perform GA analysis for obtaining the trade-off optimized tunings, where the simulation analysis was performed and compared to the performance of PSO analysis. Furthermore, the result is compared with manually calculated controller tunings. Last but not least, the conclusion is covered in Section 5.

2. Literature Review

The first systematic PID controller tuning was introduced by Ziegler-Nichols (ZN) [21], which is fixed to the single loop. The multivariable loop has involved more than one controller. It can apply a decentralized tuning approach, which enables each controller to perform control in its loop and is obtainable through detuning, sequential loop closing, simultaneous equation solving, trial-and-error and independent tuning. The authors in [22] applied sufficient condition to design the IMC multi-loop tuning method to guarantee stability for the stable filter. In [7], the authors extended Biggest-log-modulus (BLM) to classical ZN tunings by applying the detune factors to the tuned PID controller for obtaining better control performances among the interacted loops [23]. This method was further applied to three inputs and two outputs energy management systems in [24]. The authors in [25] applied uncertainty and disturbance estimator (UDE) based control method to control water level of the coupled-tank system that obtains minimum settling time and zero steady-state error.

The authors in [27] highlighted all stabilizing parametric regions under multivariable PID control structure by using Hermite-Biehler theorem, while [27] applied GA optimization to support PID controller tunings to a TITO system heavy oil molecule. Researchers in [28] analyzed the performance of improved PID control system applied to the automobile cruise control system (ACCS) by using Ant Lion Optimization (ALO). Paper [2] analyzed a design control approach to use primary controllers, auxiliary controllers, and correction numbers via the RGA tool to determine the optimal control pairs. Concurrently, paper [16]

compared the responses of RGA, Neiderlinski Index, Morari Resiliency Index, Condition Number (CN), and robustness analysis (RA) and Singular Value Decomposition methods for a multiple loop process. Furthermore, researchers in [6] proposed Sliding Mode Control (SMC) to reduce the steady-state and overshoots responses of the Heating, Ventilation, and Air Condition (HVAC) system. In other applications, authors in [3] applied a multivariable type of tracking differentiator (TD) and linear extended state observed (LESO) for reducing the total disturbance for aero-engine. Besides, [15] used Matrix A to improve the disturbance ability of a MIMO system. In detailing the literature above, it is found that the literature has demonstrated significant improvements adopted to the servo or regulatory control objectives. In fact, the performance of both control objectives could be upheld together via adopting the stochastic optimization analysis to the tested models.

Particle Swarm Optimization (PSO) is a metaheuristic optimization method used to solve optimization problems. Paper [29] applied the PSO technique to decrease overshoots with the new anti-jamming capability to the pump system operation. In paper [30], PSO has obtained the optimal weighting matrices that reduce the oscillation of pitch motion for a helicopter. Researchers [31] applied PSO to Automatic Voltage Regulator Control (AVRC) to improve the transient response and robustness against external disturbance. Meanwhile, PSO was adapted to Fuzzy controller in paper [32] for empirical parameter selection and invariances to the robot tracker that reduced overshoot and settling time. In analyzing the convergence characteristic for nonlinear constrained optimization (NCO) problem, paper [33] proposed an easy particle of PSO to improve premature convergence by diversifying the searching direction. Paper [34] analyzed the velocity and acceleration correlation vectors in PSO to improve the robotic arms' position control and obstacle avoidance. In other applications, paper [35] applied Modified Firefly Algorithm (MFA) - PSO based Fractional order PID (FOPID) controller to improve the torque and speed regulation for Brushless DC motors (BLDCMs). Besides, Paper [36] combined PSO analysis with median filter in a simulation-based experiment to improve the image quality of distorted tribal artworks, whereby the result is compared with Histogram Equalization (HE) techniques.

GA optimization analysis has been used widely to solve many complex engineering problems concerning multi-objective function Genetic Algorithm [37, 38], temperature control for boiler's superheater steam [39] and cascade control loop [40]. Researchers in [41] discussed the pros and cons and the future prospect of GA and paper [42] elaborated basic benchmarks tests and evolutionary algorithms with the respective improvements on the fitness values. Authors in [43] improved the cloud computing task scheduling via GA. Researchers in [19] extracted the requirements of a full-fledged system and developed a highly flexible GA

algorithm to obtain various solutions, improving the requirements' quality. In paper [4], the authors used CF-optimization and WCF-optimization supported by the GA to analyze the stress and fatigue damage of the reduced structural weight of the jacket offshore platform SPD19A. Researchers in paper [44] developed a hybrid teaching-learning GA (HTLGA) to solve the fuel reloading optimization by dealing with three operators: coding, crossover and mutation. Paper [45] applied hybrid GA with variable neighborhood search algorithm (GAVNS) to analyze improvements on multi-period vehicle routing problems with random pickup and delivery for heterogeneous fleet, rest area and service duration time windows of vehicles. For the boiler's application, paper [33] applied GA to determine the boiler's optimum conditions that met the indoor's temperature settings and minimized the total gas consumption. Paper [46] applied GA to develop optimized Weibull Distribution via minimization of six variables, including sampling interval, sample size, samples number in pre-maintenance, control limit width, warning control limit and subinterval in between two sampling times. It overall improved the mean total hourly cost. Authors in [47] achieved the optimum mathematical solutions for nonlinear equations (SNLs) system using a grasshopper optimization algorithm (GOA) with GA, whereas the authors in [48] obtained a global search based on the K-means clustering algorithm of hybrid GA (HGA). [49] applied GA analysis for Vendor-managed Inventory (VMI), whereby GA analysed the minimum size and number of trucks to reduce transportation costs. [50] applied GA to the modularization concept that was used in designing the engine room. GA obtained the best module by considering pipe connection numbers and pipe cost constraints.

In paper [51], the authors applied GA to obtain the best Fused Deposition Modelling (FDM) process parameters that contributes to fabricating copper-reinforced ABS components for electronics, automobiles and the aerospace industry. Paper [5] used an improved GA to optimize the operation of Thermal Energy Storage (TES) based on the established hourly operation model. Indeed, those success stories have inspired a new idea by utilizing GA optimization to analyze highly interacted TITO system controller tunings. Parameter factors such as iteration, population size and mutation rates are in-depth considered in the optimization analysis conducted using the MATLAB simulation tool. Later, the control capability is visualized via the Multi-Tank function of the LOOP-PRO software.

3. Methodology

This section describes the methodology for empirical model identification and controllers for a Two-input-Two-Output (TITO) loop, stability analysis, RGA and the proposed optimization algorithms for the analysis. Besides, the section describes the used software for validation test.

3.1. Algorithms for TITO Model and Controller

In Fig. 1, the TITO loop consists of two process models for the feedback loops and two models interact with the other loop as disturbances. Therefore, four mathematical models are presented. The output is looped back to the input and contemporaneously receives the interaction from another loop. Both outputs are shown in Eq. (1) and Eq. (2), respectively:

$$Y_1(s) = G_{p11}(s)U_1(s) + G_{p12}(s)U_2(s) \tag{1}$$

$$Y_2(s) = G_{p21}(s)U_1(s) + G_{p22}(s)U_2(s) \tag{2}$$

where, $\frac{Y_1(s)}{U_1(s)} = G_{p11}(s)$; $\frac{Y_1(s)}{U_2(s)} = G_{p12}(s)$;

$\frac{Y_2(s)}{U_1(s)} = G_{p21}(s)$; $\frac{Y_2(s)}{U_2(s)} = G_{p22}(s)$

In the vector-matrix notation, the characteristic is represented as Eq. (3):

$$Y(s) = G_p(s)U(s) \tag{3}$$

where $Y(s)$ and $U(s)$ are vectors

$$Y(s) = \begin{bmatrix} Y_1(s) \\ Y_2(s) \end{bmatrix} \quad ; \quad U(s) = \begin{bmatrix} U_1(s) \\ U_2(s) \end{bmatrix}$$

Therefore, the overall $G_p(s)$ in the transfer function matrix form is shown in Eq. (4):

$$\text{TITO model, } G_p(s) = \begin{bmatrix} G_{p11}(s) & G_{p12}(s) \\ G_{p21}(s) & G_{p22}(s) \end{bmatrix} \tag{4}$$

Transfer function of each component in vector matrix $G_p(s)$ is represented in the FOPDT model [52] as Eq. (5):

$$\text{Process FOPDT model, } G_{pij}(s) = \frac{K_{pij}e^{-\theta_{pij}s}}{(\tau_{pij}s+1)} \tag{5}$$

where, K_{pij} = Process gain; τ_{pij} = Process time constant; θ_{pij} = Process dead time; $i = 1, 2$; $j = 1, 2$

The disturbance model in vector matrix $G_d(s)$ is represented in the FOPDT model as Eq. (6):

$$\text{Disturbance FOPDT model, } G_{dij}(s) = \frac{K_{dij}e^{-\theta_{dij}s}}{(\tau_{dij}s+1)} \tag{6}$$

where, K_{dij} = Disturbance gain; τ_{dij} = Disturbance time constant; θ_{dij} = Disturbance dead time; $i = 1, 2$; $j = 1, 2$.

Besides, the respective controller models are designed to match the process characteristic, which is depicted as Eq. (7):

Controller model, $G_c(s) = \begin{bmatrix} G_{c1}(s) & 0 \\ 0 & G_{c2}(s) \end{bmatrix}$ (7)

This research applies the PI controller mode for each controlled loop that is represented as Eq. (8):

PI controller mode, $G_{Ci}(s) = K_{Ci}\left(1 + \frac{1}{\tau_{Ii}s}\right)$ (8)

where, K_{Ci} = Proportional gain; τ_{Ii} = Integral gain; $i = 1, 2$

3.2. Stability Analysis

The stability of the closed loop transfer function is developed based on the Routh-Hurwitz necessity criterion; please refer to paper [38]. The obtained characteristic equation is shown as Eq. (9):

$$\left(1 + G_{c1}G_{p11}\right)\left(1 + G_{c2}G_{p22}\right) - G_{c1}G_{c2}G_{p12}G_{p21} = 0 \quad (9)$$

For the best controller settings, the feedback control loop should be ignored by expecting the zero interactions in between two control loops, where it is expected that $G_{p12} = 0$ and $G_{p21} = 0$. Therefore, the interactive loop's stability is merely dependent on the stability of the respective individual feedback loops. Its characteristic equations are respectively shown as $\left(1 + G_{c1}G_{p11}\right) = 0$ and $\left(1 + G_{c2}G_{p22}\right) = 0$.

Through the mathematical operation, the stability margin covers the range for both Proportional gain, K_{Ci} and Integral time constant, τ_{Ii}, which is depicted in Eq. (10) and (11). When both values have the same integer as the range, the lower limit for K_{Ci} could be set as 0, while the upper limit of τ_I could be a reasonable value larger than (11).

$K_{Ci} < \frac{\tau_{pi}}{K_{pi}\theta_{pi}}$ (Upper Limit for proportional gain) (10)

$\tau_{Ii} > \frac{\theta_{pi}K_{ci}K_{pi}}{1 + K_{ci}K_{pi}}$ (Lower Limit for time constant) (11)

3.3. Relative Gain Array (RGA)

RGA is a quantitative technique developed by Bristol [8] that measures the degree of interaction between the controlled and manipulated variables. It also determines the need to pair input-output when any negative or larger elements exist in the produced RGA matrix [16], allowing the multivariable loop to improve control performance [10]. The pairing loop aims at mitigating the impact or influence from another loop by adjusting the control weight or ratio to the deviated Process Variable (PV) due to the setpoint change or imposed disturbance [9]. The RGA for a TITO loop is shown in Eq. (12)

$$\lambda = \begin{bmatrix} \lambda_{11} & \lambda_{12} \\ \lambda_{21} & \lambda_{22} \end{bmatrix} \quad (12)$$

where, λ = relative gain.

For the steady-state coupling, only the process gain of every process model is considered and allocated into the matrix structure and all elements of the matrix are in Eq. (13):

$$K = \begin{bmatrix} K_{11} & K_{12} \\ K_{21} & K_{22} \end{bmatrix} \quad (13)$$

where, $K_{11} = \frac{1}{1 - \frac{K_{21}K_{12}}{K_{22}K_{11}}}$; $K_{12} = K_{21} = 1 - K_{11}$;

$K_{11} = K_{22}$

The determination is based on the interaction of the TITO loop, which is reflected by all K values. The pairing of $K_{12} < 0$ and $K_{21} < 0$ means either the open or closed loops for that control loop will have a strong unfavorable effect on the other loop and potentially causes the oscillatory response. In this case, decouplers are needed to minimize or eliminate the interaction between two loops.

3.4. Genetic Algorithm Optimization Analysis

GA is a stochastic optimization technique that uses genetic-based mechanism to generate new solutions iteratively from the best solutions of the previous generations in the competing environment. The preliminary analysis of the search region and objective function must be obtained. The Upper and Lower bound settings determine the obtainable search region via Routh-Hurwitz stability analysis. In the optimization analysis, the algorithm randomly chooses the first generation of chromosomes. For the PI controller, a group of chromosomes comprises controller parameters $K_c\tau_I$, where $K_C = c1, c2, \dots cn$, $\tau_I = I1, I2, \dots In$ are coded (see [53]). All the chromosomes are going through the computational calculation and fitness test. The fitness test runs the objective function's algorithm to produce the performance index, J, where the formula of Integral Absolute Error (IAE) is depicted in Eq. (14):

Integral Absolute Error, IAE $= \int_0^\infty |e(t)| dt$ (14)

The lower the produced IAE value, the better the quality of the new chromosome [54] in that generation cycle. Every iteration determines the two best chromosomes to be the best children or local minima. This is then proceeded with formulating a new group of chromosomes containing the best children of the previous iteration and other randomized chosen new chromosomes. Then, the optimization analysis would repeat its iteration cycles until the global minima is obtained.

GA performs three main stages in the optimization analysis known as Selection, Crossover and Mutation [41]. In the stage of Selection, GA chooses the chromosome to be analyzed within the search region, where the above-average strings are copied in a probabilistic manner [55]. The Roulette Wheel method is applied to select chromosomes as parents. Crossover operation exchanges

the genes in between parents to form new offsprings. The offsprings inherent partially characteristic of two parents that exchanges information with each other before. In this research, the uniform crossover operator has been selected, where it will randomly choose the bit of strings among parents that improve the exploitation capability to converge and produce better offsprings in shorter period. The composition of two sample chromosomes is shown as Eq. (15) and (16).

$$\text{Parent 1: } X_1 = (X_{11} + X_{12} + \cdots + X_{1n}) \quad (15)$$

$$\text{Parent 2: } X_2 = (X_{21} + X_{22} + \cdots + X_{2n}) \quad (16)$$

The unicrossover produces the offsprings with the algorithm as shown in Eq. (17) and (18).

$$\text{Offspring 1: } Y_{1i} = \underset{\substack{\text{(Inherent 1}^{\text{st}} \\ \text{parent's genes)}}}{X_i X_{1i}} + \underset{\substack{\text{(Inherent 2}^{\text{nd}} \text{ parent's} \\ \text{genes with factor values)}}}{(1 - \alpha_i)X_{2i}} \quad (17)$$

$$\text{Offspring 2: } Y_{2i} = \underset{\substack{\text{(Inherent 1}^{\text{st}} \text{ parent's} \\ \text{genes with factor values)}}}{(1 - \alpha_i)X_{1i}} + \underset{\substack{\text{(Inherent 2}^{\text{nd}} \\ \text{parent's gene)}}}{X_{2i}} \quad (18)$$

Factor parameter of binary numbers, $\alpha = (\alpha_1 + \alpha_2 + \cdots + \alpha_n); \; \alpha \in (0,1)$

Mutation is known as the error in copying the genes. Applying this mechanism improves GA's possibility and exploration capability to create evolutionary solutions. Mutation chooses the newly produced best child in the bit of strings by flipping a few genes in it to seek any possibility of further improving the fitness of strings through minimum local searches, where the optimum values are very close to the presented best child. It can be set by applying mutation rate in the range between 0 to 1. Over setting on mutation rate can cause highly flipped of children, that will affect the attainment of the best solutions. Mutation rates could be set based on the problem's condition and search space. As the iteration continues, the $lbest$ of the new generation is repetitively is compared to $gbest$. If the varies becomes less than the fitness value, Fs the $gbest$ solution is obtained and termination criteria is trigged to cease the operation. Otherwise, the optimization analysis will keep repeating a new cycle until the maximum iteration, $MaxIt$ is met. The success and termination of optimization analysis can occur either after obtaining the maximum number of iterations or with the attainment of average fitness that is less than the best fitness [40]. Eventually, the GA analysis has obtained the best PI controller tunings for both servo and regulatory controls.

Figure 2 elaborates the pseudo code of GA optimization in relation to the imposed input settings. Stability analysis determined the range of Upper limit, UB and Lower Limit, LB. During optimization analysis, the children are to be simulated by the identified

FOPDT models to obtain IAE value. The GA analysis performed the setpoint and disturbance transfer function concurrently, which $J1$ and $J2$ are for the left tank and $J3$ and $J4$ are for the right tank. Both the chromosomes of PI controller for left and right tanks produced IAE values. The respective IAE values are summazed and compared. The smaller total integral error reflects better control performance and has a higher probability to be selected as the local best solution, $lbest$. In the if loop function, Absolute values of $lbest$ is a minus to the stage best global solution, $gbest$ for obtaining fitness value, Fs, which would trigger termination option when $\| Fs \|$ < 1e-6.

Indices:

n	number of variables
P	population size
mu	mutation rate
$MaxIt$	maximum iteration
UB	Upper limit
LB	Lower limit
J	Objective function value
Fs	fitness value
$K_{c(Left)}$	Proportional gain of left tank
$\tau_{I(Left)}$	Integral time constant of left tank
$K_{c(Right)}$	Proportional gain of right tank
$\tau_{I(Right)}$	Integral time constant of right tank
$G_{p(L)}$	Process model of left tank
$G_{d(L)}$	Disturbance model of left tank
$G_{p(R)}$	Process model of right tank
$G_{d(R)}$	Disturbance model of right tank
$lbest$	Local best
$gbest$	Global best
i	Integer number

Input

n =4; $P \in (0, 80)$; $MaxIt \in (0, 100)$; $UB \in (0, 40)$; $LB \in (0, 40)$; $\| Fs \|$ = 1e-6

Begin

 Initialize and evaluate Population $[P(0)]$

  $i \leftarrow 1;$

 Select Individual Population $[P(i)] = \{K_{c(Left)}, \tau_{I(Left)},$
        $\ldots K_{c(Right)}, \tau_{I(Right)}\}$

 Unicrossover of chromosomes. Refer Eq. (17) and (18).

 Mutation on the selected children.

 Performance test. Refer Eq. (5) and (6)

 Calculating error values,

  e1 = *1 - step* $(G_{p(L)})$

  e2 = *1 + step* $(G_{d(L)})$

  e3 = *1 - step* $(G_{p(R)})$

  e4 = *1 + step* $(G_{p(R)})$

 Integrating error values, refer to (14)

  $J1$ $= \int_0^\infty |e1(t)| dt$

$J2 \quad = \int_0^\infty |e2(t)|dt$

$J3 \quad = \int_0^\infty |e3(t)|dt$

$J4 \quad = \int_0^\infty |e4(t)|dt$

Total Integral Absolute Error, J is referred to the total number of populations, J[P]

$J[P] = J1 + J2 + J3 + J4.$

Evaluation (start with population P=1)

F_obj[1] =J[1]

F_obj[2] =J[2]

....

F_obj[P] =J[P]

Fitness

Fitness[1] = 1 / (1+F_obj[1])

Fitness[2] = 1 / (1+F_obj[2])

....

Fitness[P] = 1 / (1+F_obj[P])

Total Fitness = Fitness[1] + Fitness[2].....+Fitness[P]

Probability of each child

Probability [1] = Fitness[1] / Total Fitness

Probability [2] = Fitness[2] / Total Fitness

....

Probability [P] = Fitness[P] / Total Fitness

Selecting two children with highest Probability

$lbest = \max_J \sum_{i=1}^P Probability$

while $\| lbest \| > \| gbest \|$

$lbest = gbest$

else

endwhile

if $(\|lbest - gbest\| > 1e^{-6}$ *or* $i < MaxIt)$

$i \leftarrow i +1;$

return

else

end if

end

Output

Best solution: $\min_J \sum_{i=1}^{MaxIt} J$

$gbest = K_{c(Left)}, \tau_{I(Left)}, K_{c(Right)}, \tau_{I(Right)}.$

Fig. 2. The developed GA algorithm pseudocode.

3.5. Particle Swarm Optimization Analysis

PSO regenerates new particles in continuous iterations via random selection of new samples. The generated particles are applied to the defined objective function for determining the personal best position, P_{id} and global best position, P_{gd} [56]. Two algorithms are fundamental to the PSO analysis: random position, X_{id} and the random velocity, V_{id}, respectively, shown in Eq. (19) and (20).

Velocity update,

$$V_{id(t+1)} = WV_{id(t)} + c_1 r_1 (P_{id} - X_{id(t)} + \cdots \\ \cdots + c_2 r_2 (P_{gd} - X_{id(t)}) \quad (19)$$

Position update,

$$X_{id(t+1)} = X_{id(t)} + V_{id(t+1)}t \quad (20)$$

where, W = inertia weight, t is 1 in each interactive step, r_1 and r_2 are random values $\in (0, 1)$, c_1 and c_2 are coefficients of the particle acceleration value, which affects the convergence trend are $\in (0, 2)$, $X_{id(t)}$ is initial position, and $V_{id(t)}$ is initial velocity. In addition, the included critical settings cover lower and upper limits are set to 2 - 35 (%/m) for the K_C and $0 - 3$ (s) for τ_I, $P \in (20, 80)$ and $MaxIt \in (40, 100)$, which are adequately used for the PSO optimization analysis to the tested loop of this research.

The PSO algorithm has begins with randomly select a new group of particles, $X_{id(t)} = K_C \tau_I$, where $K_c = c1, c2, \ldots .. cn$, $\tau_I = I1, I2, \ldots \ldots I(t)$. The objective function covers process, disturbance, PID controller and integral error algorithms. While running the iteration, each particle is evaluated by the objective function that produces the respective integral error values. The tested particle with the least integral error value is $P_{id(t+1)}$, and then is compared with $P_{gd(t)}$. If the $P_{id(t+1)} < P_{gd(t)}$, $P_{id(t+1)}$ replace the existing value of $P_{gd(t)}$ to give $P_{gd(t+1)}$. Then, the analysis would repeat for the next iteration, where the $X_{id(t+2)}$ are randomly selected particles. The iteration analysis results on the convergence of the P_{gd} until the most updated P_{gd} value possess the K_C and τ_I values and the least integral error value.

3.6. The Research Simulation Tool

This research utilizes the multi-tank function of the LOOP-PRO software. Refer to [56]. The main objective is to regulate the water level in left and right tanks. It uses two PID controller tunings respectively for the independent closed-loop control of both tanks. On the servo control, the setpoint tracking performance is tested by adjusting the setpoint of each control loop between the level 2m − 3m − 2m. Adjustment on the setpoint regulates the control valve's opening and changes the water flow rate to the controlled tank. However, it also affects the channel of water flow to another tank. On the regulatory control, the disturbance rejection performance is tested by adjusting the outflow water rate between 1 m³/min - 2 m³/min - 1 m³/min, via adjusting the hand valve located at the bottom of both left and right tanks. Adjustment on the opening of the hand valve changes the water level in the tank and consequence changes of control action to control water inflow to the tank and concurrently affects the channeled water flow to the other tank.

4. Analysis and Result Discussion

This section explains the obtained FOPDT models, RGA, and stability analysis of the multi-tank function. It is followed by developing the Simulink model and determining PID controller tunings for both left and right tanks. Analysis of criteria settings has been conducted to GA optimization analysis and the reliability of GA-based optimization analysis is compared with PSO analysis. At last, all generated process responses from various tuning methods are described, whereby the performance of GA-based tunings is discussed and finalized.

4.1. Empirical Model Identification

Empirical model identification for the multi-tank function of the LOOP-PRO software is directly obtained from this software after conducting the open loop test. The obtained models consist of process and disturbance models for both left and right tanks. All the identified models are listed in Table 1.

Table 1.   Dynamic models of the left and right tanks.

Model	Left Tank	Right Tank
Process Model	FOPDT, LL $= \dfrac{0.06e^{-7.1s}}{13.05s + 1}$	FOPDT, RR $= \dfrac{0.063e^{-6.8s}}{14.28s + 1}$
Process Model (interaction from the other tank)	FOPDT, RL $= \dfrac{0.035e^{-5.8s}}{14s + 1}$	FOPDT, LR $= \dfrac{0.03e^{-7.49s}}{14.11s + 1}$
Disturbance Model (external)	FOPDT (Dist $-$ L) $= \dfrac{-0.3512}{3.543s + 1}$	FOPDT (Dist $-$ R) $= \dfrac{-0.408}{4.811s + 1}$

4.2. Relative Gain Array and Stability Analysis

The steady-state coupling only considers each model's process gain, refer to Eq. (13), therefore the arrangement of gains is shown in matrix form as below:

$$K= \begin{bmatrix} 0.06 & 0.03 \\ 0.035 & 0.063 \end{bmatrix}$$

where, $K_{11} = \dfrac{1}{1-\frac{(0.03)(0.035)}{(0.06)(0.063)}} = 1.3846$

As referred to the Eq. (13), the calculation determines the new RGA value in matrix form shown as

$$\text{RGA}, K= \begin{bmatrix} 1.3846 & -0.3846 \\ -0.3846 & 1.3846 \end{bmatrix}$$

Both K_{12} and K_{21} are < 0, implying that the control loop would significantly impact another loop. Therefore, a proper pairing or decoupler for compensating the interacted loop is unavoidable.

For the stability analysis, substituting FOPDT's parameters of Table 1 into Eq. (10) and (11) yielded the

stability margin of the left tank as $K_c < 30.46$ and $\tau_I > 8.45$, while the right tank as $K_c < 35.0$ and $\tau_I > 9.82$. Incorporating the UB and LB settings range give the most appropriate stability margin of $K_c < 30.46$ and $\tau_I > 9.82$, allowing the GA to analyse the best PI controller settings for both left and right tanks.

4.3. PID Tunings of Multi-tank Function for the Performance Analysis

Table 2 tabulates various PI controller tuning methods. All tuning methods applied the two decouplers-based decentralised multivariable control scheme. It covers IMC-Moderate tunings, followed by ZN tuning scheme with detuning factors (F_T) of 0.8, 1.0 and 1.2. Furthermore, the PI controller tunings of GA optimization analysis is listed for comparison with other tuning methods.

The tuning of PI controllers for both left and right tanks are conducted simultaneously. In operation, both loops for left and right tanks are operating and is connected with each other. The parameter changes of one loop will affect the performance of the other loop, whereby the PI controller of the other loop will react to the changes in maintaining stability control of that loop. Therefore, all the pair of PI controller settings in Table 2 are simultaneously applied to the TITO system, including the GA_Optim. tunings.

Table 2.   PI controller tunings for left and right tanks.

Tuning Method	PI Tunings (Left Tank)		PI Tunings (Right Tank)	
	$K_{C(Left)}$, %/m	$\tau_{I(Left)}$, min	$K_{C(Right)}$, %/m	$\tau_{I(Right)}$, min
IMC_ Moderate	3.42	13.00	3.71	14.26
ZN_F_T =0.8	34.5	18.96	37.5	18.16
ZN_F_T =1	27.6	23.7	30	22.7
ZN_F_T =1.2	21.23	30.81	23.08	29.51
GA_Optim.	20.47	15.54	22.03	16.55

4.4. Simulink Model for Simulation Analysis

Simulation analysis was performed in the SIMULINK of the MATLAB simulation tool. Figure 3 shows the design of TITO control loop with the developed decouplers to mitigate the interaction among the left and right tanks. Besides, it shows the position of process and disturbance models in the overall control loops. Meaning to say that the dynamic process will have one FOPDT model for the process and another FOPDT model reflects the behaviour of system after the disturbance is imposed. The setpoint change can be performed by applying step unit signal to port 2 or 3, whereas the disturbance imposes a unit step signal to port 1 or 4. The process response is obtained from ports 3 to 7.
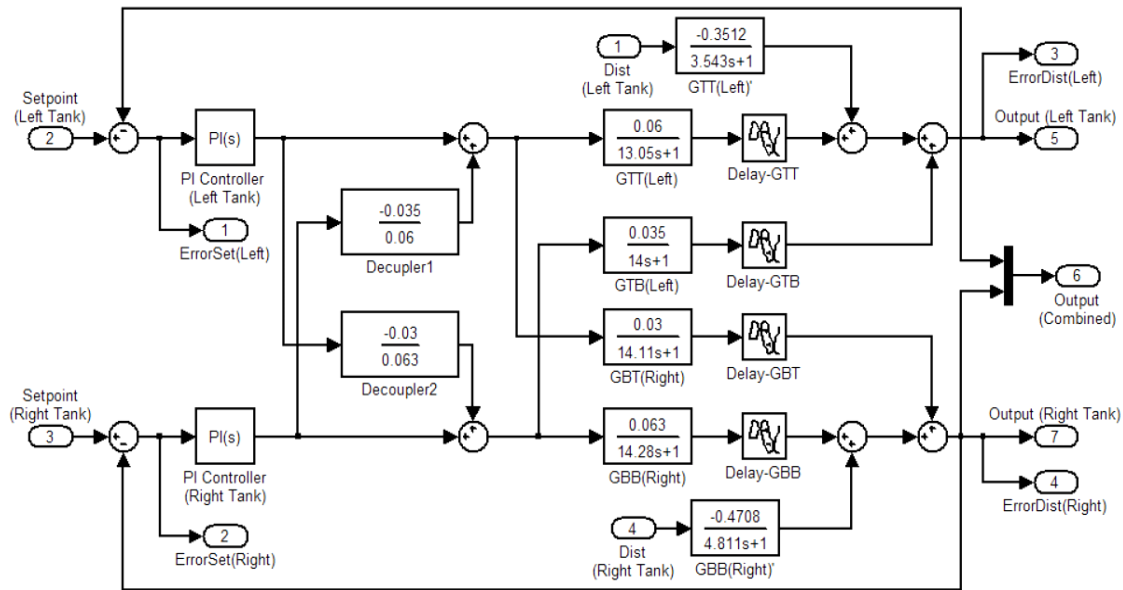
Fig. 3. Simulink model of multi-tank process with decouplers.

4.5. Analysis of Criteria Settings for Iteration ($MaxIt$), Population (P) and Mutation Rate (mu)

As referred to Fig. 2, the analysis of $MaxIt$, P and mu are conducted by rating the $MaxIt$ at 40, 80 and 100, where the best solution (integral absolute error values) from the respective populations is observed. It helps to clarify the best criteria setting for GA analysis on the tested multi-tank function, which FOPDT models have identified.

Figure 4(a) illustrates the obtained best solution for the $MaxIt$ of 40 while the P and mu are increasing. It is found that the mu of 0.02 is not adequately used because it has generally produced higher integral error values, therefore the poorer solutions compared to other settings. Besides, it's seemed that increasing mu improves the best solutions (smaller total integral error values). However, the rate of improvement has been reduced after the $MaxIt = 40$. The P of 20 - 40 and mu of 0.1 - 0.14 can be considered for this iteration.

Figure 4(b) illustrates the best solution for the $MaxIt = 80$ in varying the P and mu. Regardless of mu, overall GA analysis obtains very close total integral error values as the P exceeds more than 40. This is particularly true for the mu of 0.1 (population=40), which produces the best solution compared with other mutation rates. However, mu of 0.02 is less preferably used for the GA analysis because the solutions are much biasing in $P < 10$.

Figure 4(c) depicts the GA analysis of $MaxIt = 100$ in varying the P and mu. The figure shows that overall best solutions are very close after $P > 40$. A mu of 0.06 to 0.14 could be used for the GA analysis. However, the $mu = 0.02$ is not considered due to higher J values.

As referring to the findings of GA to the tested model, it is noted that the $P = 40$ can be selected as the best choice for the GA analysis, where the resultant J as shown in Fig. 4(b) and 4(c) have less variation even afterward the larger $MaxIt$ has been used for GA analysis to the multi-tank system. Figures 4(b) and 4(c) also show that all the produced J from the variation of $MaxIt$ and mu has accumulated at one point for $P = 80$, which means that this point is adequate to obtain a consistent result for GA optimization analysis. Further extending the P is not improving the result but more time- consuming. Therefore, the analysis of the P value for $MaxIt = 100$ was not further extended to 100. Besides, the larger $MaxIt$, the more extended period is needed for the GA analysis. The obtained $MaxIt = 40$ in Fig. 4(a) seems unable to obtain the best solutions in overall. Nevertheless, the $MaxIt = 100$ is considered too time-consuming as reflected in Fig. 4(c) that the obtained J has stabilised after the $MaxIt = 40$. Therefore, $MaxIt = 80$ is preferably selected as compared to 40 and 100. In addition, $mu = 0.1$ seems to produce more consistent results for various iterations and mutation rates and therefore is selected for the GA analysis to the developed FOPDT models.
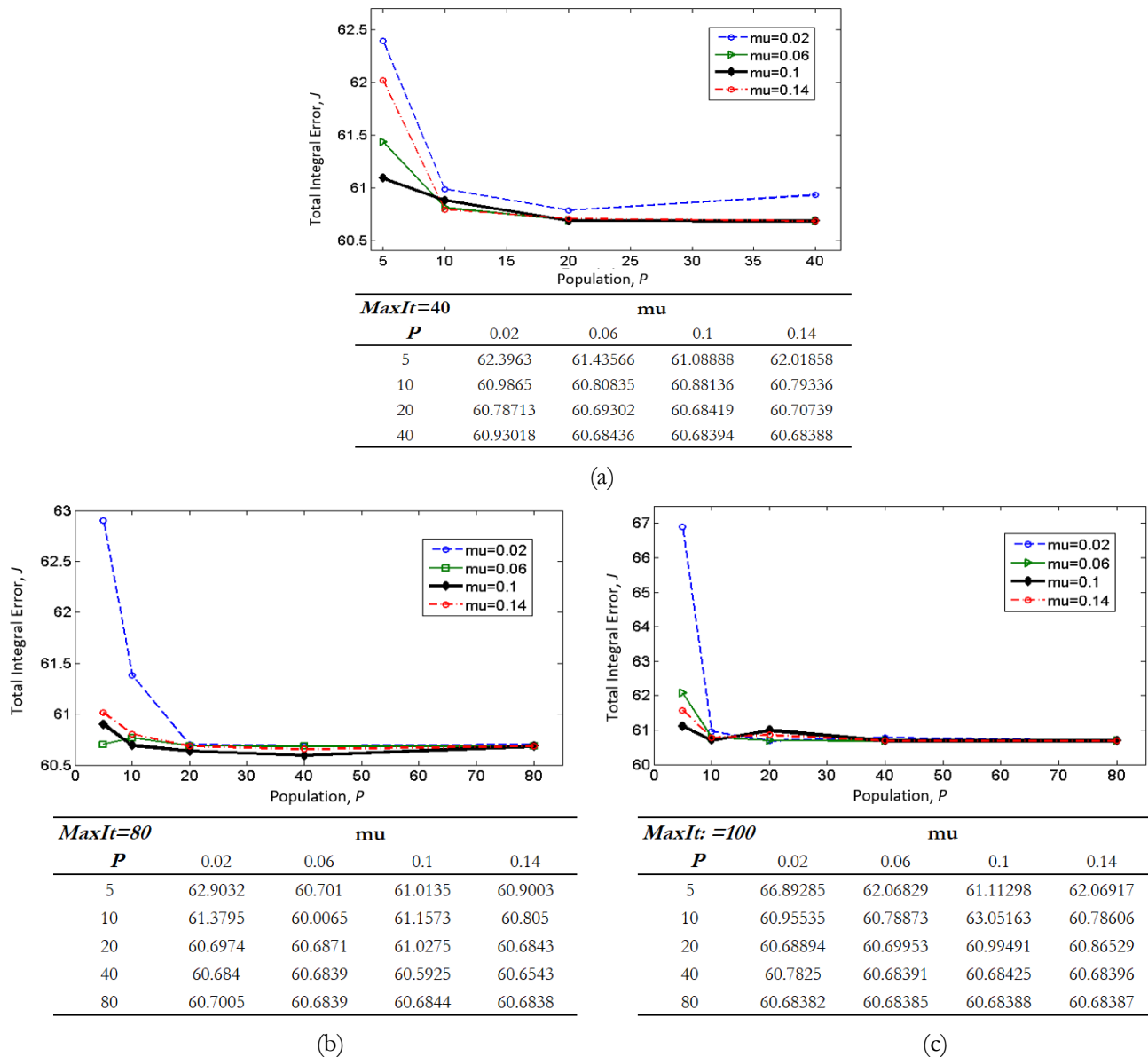
MaxIt=40		mu		
P	0.02	0.06	0.1	0.14
5	62.3963	61.43566	61.08888	62.01858
10	60.9865	60.80835	60.88136	60.79336
20	60.78713	60.69302	60.68419	60.70739
40	60.93018	60.68436	60.68394	60.68388

(a)

MaxIt=80		mu		
P	0.02	0.06	0.1	0.14
5	62.9032	60.701	61.0135	60.9003
10	61.3795	60.0065	61.1573	60.805
20	60.6974	60.6871	61.0275	60.6843
40	60.684	60.6839	60.5925	60.6543
80	60.7005	60.6839	60.6844	60.6838

(b)

MaxIt: =100		mu		
P	0.02	0.06	0.1	0.14
5	66.89285	62.06829	61.11298	62.06917
10	60.95535	60.78873	63.05163	60.78606
20	60.68894	60.69953	60.99491	60.86529
40	60.7825	60.68391	60.68425	60.68396
80	60.68382	60.68385	60.68388	60.68387

(c)

Fig. 4. GA analysis on the obtained total integral error for (a) $MaxIt = 40$; (b) $MaxIt = 80$; and (c) $MaxIt = 100$.

4.6. Comparison on Control Performance of GA and PSO Optimization Analysis

The simulation analysis of control performance is compared between GA and PSO tunings. It is obtained by simulating the developed FOPDT models in Fig. 3 with the controller tunings from the respective tuning values produced by GA and PSO analysis. Servo and regulatory controls are implemented. The process reaction and interaction response from other tanks are obtained via simulation analysis are shown in Fig. 5.

Figure 5(a) depicts the unit setpoint change is applied to the left tank. Control action drives the PV to a new set level and produces disturbance to the interacted right tank. Both GA and PSO tunings produce consistent response curves when PV is driven to the new set level. Fortunately, the impact to the right tank is minimal and consistent in applying either GA or PSO analysis for controller tunings. In Fig. 5(b), the unit setpoint changes at the right tank drive the PV to the new set level. GA tuning has performed better than PSO analysis because it

does not produce the additional overshoots at the right tank. For the disturbance to the left tank, GA reacted reasonably in maintaining the PV without significant oscillations.

Figure 5(c) depicts the response of the developed models that react to the applied unit disturbance to the left tank. Both GA and PSO tunings perform reasonably in responding to the disturbance of the left tank. For the interaction to the right tank, it is noted that PSO converges faster than GA in driving the PV back to the initial load level. Figure 5(d) above depicts the responses of the developed TITO module after being imposed by a unit disturbance to the right tank. For the reaction to the disturbance, both GA and PSO tunings produce slight oscillations, and surprisingly it is found that PSO tunings produce more oscillations than GA tunings. Besides, the response curve due to interaction to the left tank shows that PSO produces responses faster than the GA tunings. However, PSO tunings also produced overshoots in same response. Overall, it is found that the process

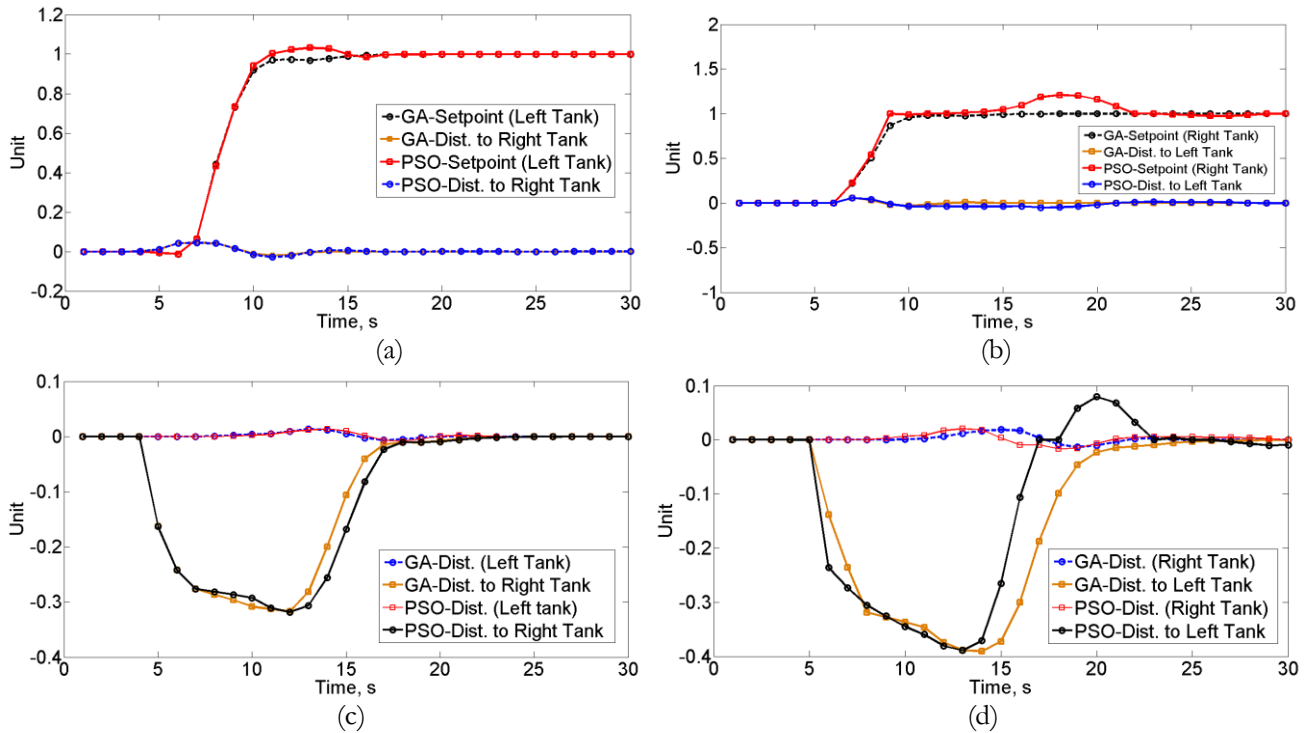response of GA is better than PSO tuning for multi-tank function of TITO system with FOPDT models.

(a)

(b)

(c)

(d)

Fig. 5. Setpoint change and disturbance for GA and PSO (a) Left tank (setpoint); (b) Right tank (setpoint); (c) Left tank (disturbance); d) Right tank (disturbance).

4.7. GA Performance Analysis for Multi-tank Function

The performance analysis discusses the output response curve, settling time and integral error values to the tested multi-tank function in servo or regulatory control objectives. It reflects the sustainability of GA analysis to improve the control performance. Both servo and regulatory controls were applied by changing the water level setpoint between $2m - 3m - 2m$ and imposed load change between $1m^3/min - 2m^3/min - 1m^3/min$. The produced output responses, settling time and IAE values are then recorded.

Figure 6(a) compares the output responses of various PI controller settings in controlling the left tank. The responses show that GA-Optim. produced more consistent control action to drive PV to the new setpoint within shortened period and fewer oscillations at the output response. Figure 6(b) elaborates the produced response of the left tank resulting from the changes of control action from the right tank. The left tank accepts the changes as a disturbance, whereby disturbance rejection performance among various tuning methods is compared. Respective settling times and IAE values are tabulated in Table 3. For the column Setpoint Changes of Left Tank, the produced overshoots and steady-state error (SSE) are also tabulated for more apparent observation.
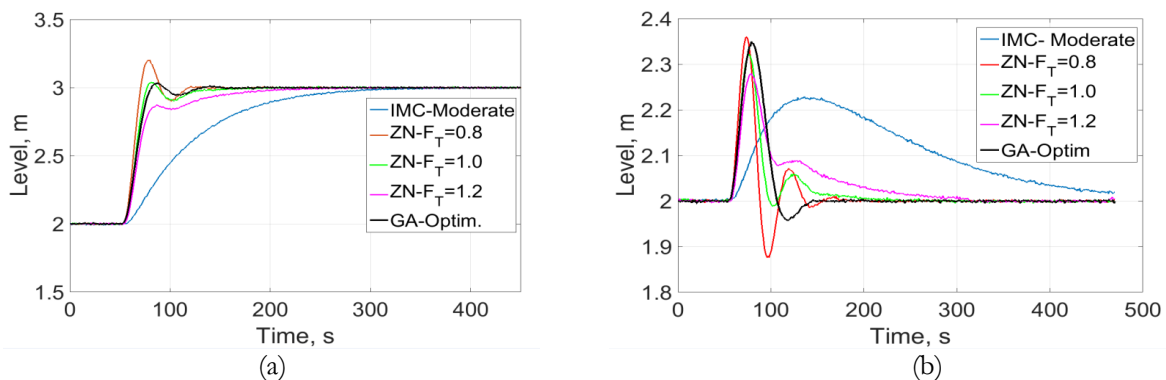

(a)

(b)

Fig. 6. Left Tank - setpoint change and reaction to the disturbance (a)Setpoint changes 2m - 3m; (b) Disturbance from the right tank.

Table 3. Performance analysis for the left tank.

Tuning Method	Setpoint Changes of Left Tank				Disturbance from the Right Tank	
	IAE	Settling Time(s)	Over shoot (%)	SSE	IAE	Settling Time(s)
IMC-Moderate	87.74	293	0	0.000	30.81	454
ZN-F_T =0.8	16.32	113	20.05	0.001	5.184	131
ZN-F_T =1	19.85	144	3.79	0.000	6.96	143
ZN-F_T =1.2	33.49	196	0	0.001	11.77	231
GA-Optim.	16.21	121	3.29	-0.001	5.689	130

It is found that the IAE value of the GA-Optim. is slightly higher than ZN-F_T = 0.8, but both tuning methods have a very close settling time. The overall result shows that GA-Optim. are the best controller tunings for the left tank's servo and regulatory control objectives.

Figure 7(a) implied the output response to the right tank in reflecting the disturbance rejection performance due to the load changes from the left tank. GA-Optim. tunings seem to perform no better than IMC-Moderate because some overshoots are produced to maintain the PV at the setpoint value. On the other hand, Fig. 7(b)

compares the output response of the servo control by applying various PI controller tunings to the right tank. However, IMC-Moderate tuning reacts slowly in the servo control operation, which gives a longer settling time. The overall comparison depicts that GA-Optim. tuning for the right tank produces the best performance in considering together both servo and regulatory controls.

The respective settling time and IAE values are depicted in Table 4. For the column Setpoint Changes of Right Tank, the produced overshoots and steady-state error (SSE) are also tabulated for more apparent observation. It is found that the reaction of IMC-Moderate to the interaction from the left tank is very weak, where the indicator shows no oscillation but prolong settling time. Overall, the IAE value and settling time of the GA_Optim. are closer to the ZN-F_T = 1 tunings. Still, GA_Optim. demonstrates better results, credited to the least settling time and IAE value. Moreover, it is found that GA_Optim. has produced a curve response with more degree of improvements as compared to all other manually calculated controller tunings. Therefore, the overall comparison shows that GA_Optim. tunings have better controllability to the right tank of the multi-tank function.

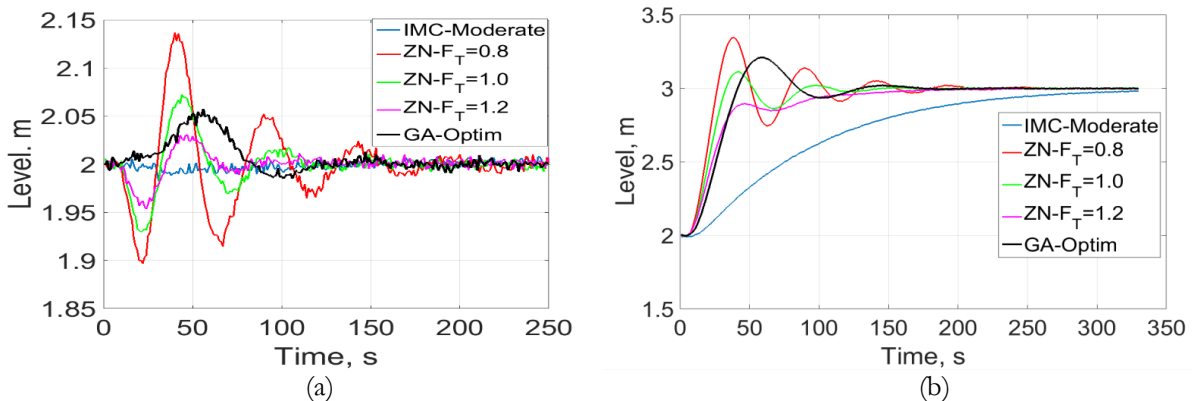(a)   (b)

Fig. 7. Right Tank – Reaction to the disturbance and setpoint change (a) Disturbance from the left tank; (b)Setpoint changes 2m - 3m.

Table 4. Performance analysis for the right tank.

Tuning Method	Disturbance from the Left Tank		Setpoint Changes of the Right Tank			
	IAE	Settling Time(s)	IAE	Settling Time(s)	Over shoot (%)	SSE
IMC-Moderate	4.252	0	84.53	326	0	0.016
ZN-F_T = 0.8	6.824	144	16.96	176	34.36	0.002
ZN-F_T = 1	7.827	75	16.63	128	11.31	0.002
ZN-F_T = 1.2	13.23	54	28.11	160	0	0.001
GA-Optim.	6.743	72	15.76	121	20.88	0.002

Figures 8(a) and 8(b) imply the responses of the external disturbance to water level measurement of left and right tanks. All the controller tunings reacted speedily to the imposed disturbances except for the IMC-Moderate tuning, in which the disturbance rejection capability is weak in Fig. 8(a), but the response is worse in Fig. 8(b). Output response curve drives slowly for both servo and regulatory controls. Among all controller tunings, GA-Optim. produced the least oscillatory and shortened settling time than other tuning methods. ZN-F_T = 0.8 tunings reacted the most aggressively but did not seem to significantly contribute to the resultant response when it was compared with GA-Optim tunings.

(a)   (b)
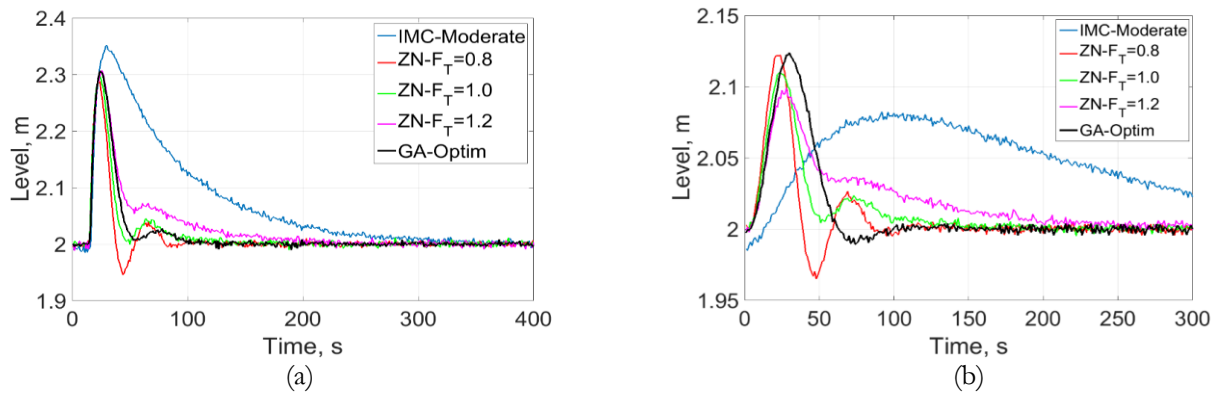
Fig. 8. Both left and right tanks - Reaction to the external disturbance (a) Disturbance to the left tank; (b) Disturbance to the right tank.

Table 5. Disturbance rejection performance for both tanks.

Tuning Method	Left Tank		Right Tank	
	IAE	Settling Time (s)	IAE	Settling Time (s)
IMC-Moderate	0.1532	225	6.587	>300
ZN-F_T = 0.8	1.348	77	0.7329	72
ZN-F_T = 1	0.7028	84	0.3898	79
ZN-F_T = 1.2	0.4113	134	0.2689	107
GA-Optim.	0.7857	83	0.3846	54

The respective settling time and IAE values are depicted in Table 5. On average, GA-Optim. has a closer settling time but a lower IAE value than ZN-F_T = 0.8 tunings. ZN-F_T = 1.2 tunings produced the least IAE value; however, settling time was dragged very much compared with GA-Optim. tuning. Therefore, the

analysis result reflected that PI controller tunings of GA-Optim. have better controllability to the closed-loop control for both left and right tanks.

Overall, the integral error values are cumulatively compared as in Table 6. The IMC-Moderate tuning possesses the largest IAE values, followed by the ZN-F_T = 1.2, ZN-F_T = 1.0 and ZN-F_T = 0.8 tunings. The GA-Optim. tunings produced the response with the least integral error values and approximately 78% improved performance compared to IMC-Moderate tunings. In addition, GA-Optim. also showed the consistency improvement on the IAE value to various ZN tuning schemes. Even the IAE value of GA-Optim. is close to ZN-F_T = 0.8, the PI controller tunings of GA-Optim. is still the best tuning because of fewer oscillation responses as depicted in Fig. 8(a) and Fig. 8(b).

Table 6. IAE values for various control tuning methods.

PI Tuning Method		IAE (Setpoint)	IAE (Dist. to Left)	IAE (Dist. to Right)	External Disturbances	Total IAE
IMC-Moderate	Left Tank	87.74	-	30.81	0.1532	214.07
	Right Tank	84.53	4.252	-	6.587	
ZN-F_T=0.8	Left Tank	16.23	-	5.184	1.348	47.28
	Right Tank	16.96	6.824	-	0.7329	
ZN-F_T=1	Left Tank	19.85	-	6.96	0.7028	52.36
	Right Tank	16.63	7.827	-	0.3898	
ZN-F_T=1.2	Left Tank	33.49	-	11.77	0.4113	87.28
	Right Tank	28.11	13.23	-	0.2689	
GA-Optim.	Left Tank	16.21	-	5.689	0.7857	45.57
	Right Tank	15.76	6.743	-	0.3846	
Improvement by using GA-Optim. compared to IMC-Moderate (%)						**78.74**

GA Optimization analysis is better than manually calculated controller tunings in obtaining the PI controller tunings. Credit to the applied stochastic optimization technique that chooses the best tuning values in every iteration process and further produces better tuning values as the optimization is proceeding. The analysis mechanism selects the best solutions of previous generations to seek further improvements in future iteration until the analysis is terminated. Therefore, it gives a better opportunity to obtain the PI controller tunings using the optimization technique than the manually calculated controller tunings, where the result only relies on the mathematical formulas.

5. Conclusion

Manually calculated control tunings for the multivariable loop are challenging and even not guaranteed satisfactory performance because of the existing interaction among loops and external disturbances. This research presents a systematic analysis using computational optimization techniques to support regular tuning practices by applying the trade-off controller tuning fixed to transient and steady-state responses of TITO control loop with the identified FOPDT model. Initially, the RGA analysis was conducted to clarify the need for decoupler or feedforward compensation to the controlled loop. Stability analysis determines the bound settings of the GA optimization analysis, which includes $K_c < 30.46$ and $\tau_I > 9.82$. Analysis on the GA's setting criteria to the tested models has shown that the $MaxIt = 80$, $P = 40$ and $mu = 0.1$ gives the most effective analysis in term of achieved results and period. While comparing the GA's response performance with other tuning methods, PI controller settings of GA produced the better output responses, IAE values and settling time. The performance analysis was conducted to the multi-tank function of LOOP-PRO software. The optimized PI control settings for the left tank are $K_{C(Left)} = 20.471$ %/m and $\tau_{I(Left)} = 15.54$ s. At once, the optimized PI control settings for the right tank are $K_{C(Right)} = 22.026$ %/m and $\tau_{I(Right)} = 16.553$ s. It is found that GA optimization analysis yielded the best PI controller tunings for both servo and regulatory controls. In the best scenario, the improved control performance by applying GA analysis obtains 78.74 % as compared to IMC-Moderate tuning for the same multivariable model.

References

[1] R. Claub, T. Pursche, and B. Tibken, "Multivariable control of a heat pump system based on a local linear model network," in *57th Annual Conference of the Society of Instrument and Control Engineers of Japan*, Nara, Japan, 2018, pp-1110-1115.

[2] P. Navratil, L. Pekar, and R. Matusu, "Control of a multivariable system using optimal control pairs: A quadruple-tank process," *IEEE Access*, vol. 8, no. 1, pp. 2537-2563, Jan. 2020.

[3] Y. Li, X. Du, X. Sun, A. Dai, and J. Chen, "Multivariable control for aero-engine based on active disturbance rejection control," in *38th Chienese Control Conf.*, Guangzhou, China, 2019, pp. 773-778.

[4] G. I. Tsoumalis, Z. N. Bampos, G. V. Chatzis, P. N. Biskas, and S. D. Keranidis, "Minimization of natural gas consumption of domestic boilers with convolutional, long-short term memory neural networks and genetic algorithm," *Applied Energy,* vol. 299, p. 117256, 2021.

[5] Z. Wang, L. Cao, and H. Si, "An improved genetic algorithm for determining the optimal operation strategy of thermal energy storage tank in combined heat and power units," *Journal of Energy Storage*, vol. 43, pp.1-9, Nov. 2021.

[6] A. Shah, D. Huang, and T. Huang, "Dynamic modelling and multivariable control of buildings climate by using sliding mode control," *2020 IEEE Int. Conf. on Artificial Intelligence and Information Systems (ICAIS)*, Dalian, China, March 20-22, 2020, pp 552-555.

[7] T. R. Biyanto, N. A. Sordi, N. Sehamat, and H. Zabiri, "PID multivariable tuning system using BLT method for distillation column," *IOP Conf. Series: Material Sci. and Eng.*, vol. 458, pp. 1-8, Dec. 2018.

[8] S. Thulasi dharan, K. Kavyarasan, and V. Bagyaveereswaran, "Tuning of PID controller using optimization techniques for a MIMO process," *IOP Conf. Series: Material Sci. and Eng.*, vol. 263, pp1-17, Nov. 2017.

[9] Q. Bu, J. Cai, Y. Liu, M. Cao, L Dong, R. Ruan and H. Mao, "The effect of fuzzy PID temperature control on Thermal behavior analysis and kinetics study of biomass microwave pyrolysis," *Journal of Analytical and Applied Pyrolysis,* vol. 158, pp. 1-8, Sept. 2021.

[10] M. R. Rani, "Multi-objective optimization of PID parameters using genetic algorithm," M.S. thesis, Faculty of Elec. Eng., Universiti Teknologi Malaysia, Johor, Malaysia, 2012.

[11] R. Katebi, "Robust multivariable tuning methods," in *PID Control in the Third Millennium*. London: Springer, UK, 2012, pp. 255-280.

[12] D. Castellanos-Cardenas, F. Castrillon, R. E. Vasques, and C. Smith, "PID tuning method based on IMC for inverse-response second order plus dead time processes," *Processes*, vol. 8, no. 9, pp. 1-24, Sept. 2020.

[13] I. M. Chew, F. Wong, A. Bono, J. Nandong, and K. I. Wong, "Computational optimization analysis of feedforward plus feedback control scheme for boiler system," in *Computational Science and Technology—Lecture Notes in Electrical Engineering*, R. Alfred, Y. Lim, A. Ibrahim, P. Anthony, Eds. Singapore: Springer, Aug. 2018, vol 481, pp. 97-106.
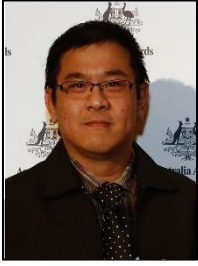
[14] N. Mahenshwari, N. Jain, A. Jingar, and M. Suthar, "Design and analysis of PID controller for CSTR process," *Int. J. of Sci. Eng. and Tech. Research.,* vol. 5, no. 2, pp. 600-603, Feb. 2016.

[15] Q. Jin and S. Wang, "Multivariable control with changed interaction for disturbance rejection," in *10th Int. Conf. on Intelligent Human-Machine Systems and Cybernetics,* Hangzhou, China, 2018, pp. 284-288.

[16] P. Juneja, A. Sharma, V. Joshi, H. Pathak, S. Kumar Sunori, and A. Sharma, "Delayed complex multivariable constrained process control—A review," in *2nd Int. Conf. on Advances in Computing Communication Control and Networking.* Greater Noida, India, 2020, pp. 569-573.

[17] K. S. Tsakalis and S. Das, "Identification for PID control," in *PID Control in the Third Millennium.* London: Springer, London, 2012, pp. 293-304.

[18] L. Desborough and R. Miller, "Increasing customer value of industrial control performance monitoring— Honeywell experience," in *6th AIChE Int. Conf. on Chemical Process Control,* AIChE Symp., J. B. Rawlings, B. A. Ogunnaike, and J. W. Eaton, Eds. AIChE, New York, 2002, Series 326, pp. 172-192.

[19] D. A. Dopazo, V. M. Pelayo and G. G. Fuster, "An automatic methodology for the quality enhancement of requirements using genetic algorithms," *Information and Software Tech.,* vol. 140, pp 1-10, Dec. 2021.

[20] E. Parra, J. L. de la Vara, and L. Alonso, "Analysis of requirements quality evolution," in *40th Int. Conf. on Software Eng.: Companion Proceedings (ICSE '18),* New York, USA, 2018, pp. 199-200.

[21] J. G. Ziegler and N. B. Nichols, "Optimum settings for automatic controllers," *Transactions of the ASME,* vol. 64, pp. 759–768, 1942,

[22] C. G. Economou, M. Morari, and B. O. Palsson, "Internal model control: Extension to nonlinear system," *Industrial & Engineering Chemistry Process Design and Development,* vol. 25, no. 2, pp. 403-411, Apr. 1986.

[23] C. Besta and M. Chidambaram, "Tuning of multivariable PI controllers by BLT method for TITO systems," *Chemical Engineering Communications,* vol. 203, no. 4, pp. 527-538, Jan. 2016.

[24] A. B. Ghazali, "A PID de-tuned method for multivariable systems, applied for HVAC plant," *IOP Conf. Series: Material Sci. and Eng.,* vol. 88, no. 1, pp. 1-7, Sept. 2015.

[25] P. Barat and S. Mandal, "Robust control of coupled-tank system using uncertainty ABD disturbance estimator," *2021 IEEE Second Int. Conf. on Control, Measurement, and Instrumentation (CMI),* Kolkata, India, 2021, pp. 128-132.

[26] X. Luan, Q. Chen, P. Albertos, and F. Liu, "Stabilizing parametric region of multiloop PID controller for multivariable systems based on equivalent transfer function," *Mathematic Problems in Engineering,* pp. 1-7, May 2016.

[27] W. Alharbi and B. Gomm, "Genetic algorithm optimization of PID controllers for a multivariable process," *Int. J. of Recent Contributions from Eng., Sci. & IT (iJES),* vol. 5, no. 1, pp. 77-96, Mar. 2017.

[28] R. Pradhan, S. K. Majhi, J. K. Pradhan, and B. B. Pati, "Performance evaluation of PID controller for an automobile cruise control system using Ant Lion Optimizer," *Engineering Journal,* vol. 21, no. 5, pp. 347-361, Sept. 2017.

[29] S. Yang and C. Gong, "Application of fuzzy neural network PID algorithm in oil pump control," in *Proceedings of the 2019 Int. Conf. of Computer Network, Electronic and Automation,* Xi'an, China, 2019, pp. 415-420.

[30] G. Yu and P. Hsieh, "Optimal design of helicopter control systems using particle swarm optimization," in *Proceedings of the Int. Conf. on Industrial Cyber Physical System,* Taipei, Taiwan, 2019, pp. 346-351.

[31] V. Kumar and V. Sharma, "Automatic voltage regulator with particle swarm optimized model predictive control strategy," in *Proceedings of the Int. Conf. Measurement, Instrumentation, Control and Automation,* Kurukshetra, India, 2020, pp. 1-5.

[32] X. Ren, Y. Yang, G. Long, J. Chen, T. Mei, J. Yu, and Q. Han, "Research on robot tracking of book returning to bookshelf based on the particle swarm optimization fuzzy PID control," in *Proceedings of the Chinese Control and Decision Conference,* Hefei, China, 2020, pp. 2507-2511.

[33] H. Tseng, P. Chu, H. Lu, and M. Tsai, "Easy Particle Swarm Optimization for nonlinear constrained optimization problems," *IEEE Access,* vol. 9, 2021, pp. 1-11.

[34] G. Rossides, B. Metcalfe, and A. Hunter, "Particle Swarm Optimization—An adaptation for the control of robotic swarms," *Robotics,* vol. 58, pp. 1-21, Apr. 2021.

[35] B. Naidu Kommula and V. Reddy Kota, "Design of MFA-PSO based Fractional order PID controller for effective torque controlled BLDC motor," *Sustainable Energy Technologies and Assessments,* vol. 49, pp. 1-8, Feb. 2022.

[36] M. Kaur and M. K. Dutta, "Restoration and quality improvement of distorted tribal artworks using Particle Swarm Optimization (PSO) technique along with nonlinear filtering," *Optik-Int. J. for Light and Electron Optics,* vol. 246, pp. 1-10, Nov. 2021.

[37] R. Valarmathi, P. R. Theerthagiri, and S. Rakeshkumar, "Design and analysis of genetic algorithm based controllers for nonlinear liquid tank system," in *IEEE-Int. Conf. On Advances in Eng., Sci. And Management (ICAESM -2012),* Nagapattinam, Tamil Nadu, 2012, pp. 616-620.

[38] I. M. Chew, F. Wong, A. Bono, J. Nandong, and K. I. Wong, "Genetic Algorithm Optimization analysis for temperature control system using cascade control loop model," *Int. J. of Computing and Digital Systems,* vol. 9, no. 1, pp. 119-128, Jan. 2020.

[39] A. Y. Begum and G. V. Marutheeswar, "Genetic Algorithm based tuning of controller for

superheater steam temperature control," *International Journal of Control Theory and Applications*", vol. 10, no. 16, pp. 57-65, 2017.

[40] I. Kaya and M. Nalbantoğlu, "Simultaneous tuning of cascade control design using Genetic Algorithm," *Electrical Eng.*, vol. 98, pp. 299-305. May 2016.

[41] S. Katoch, S. S. Chauhan, and V. Kumar, "A review on Genetic Algorithm: Past, present, and future," *Multimedia Tools and Applications*, vol. 80, no. 4, pp. 8091–8126, Feb. 2021.

[42] W. K. Wong and C. I. Ming, "A review on metaheuristic algorithms: recent trends, benchmarking and applications," in *7th Int. Conf. on Smart Computing & Communications (ICSCC)*, Sarawak, Malaysia, 2018, pp.1-15.

[43] Y. Fang, X. Xiao, and J. Ge, "Cloud computing task scheduling algorithm based on improved genetic algorithm," in *IEEE Information Technology, Networking, Electronic and Automation Control Conf. (ITNEC 2019)*, Chengdu, China, 2019, pp. 852-856.

[44] Z. Li, J. Huang, J. Wang and M. Ding, "Development and application of hybrid teaching-learning genetic algorithm in fuel reloading optimization," *Progress in Nuclear Energy,* vol. 139, pp 1-12, Sept. 2021.

[45] K. Kamsopa, K. Sethanan, T. Jamrus, and L. Czwajda, "Hybrid Genetic Algorithm for multi-period vehicle routing problem with mixed pickup and delivery with time window, heterogeneous fleet, duration time and rest area," *Engineering Journal*, vol. 25, no. 10, pp. 71-86, Oct. 2021.

[46] P. Charongrattanasakul and A. Pongpullponsak, "Optimizing the cost integrated model for fuzzy failure Weibull distribution using genetic algorithm," *Engineering Journal*, Vol 21, no. 5, pp. 253-268, Sept. 2017.

[47] M. A. El-Shorbagy, and A. M. El-Refaey, "Hybridization of grasshopper optimization algorithm with genetic algorithm for solving system of non-linear equations," *IEEE Access*, vol. 8, pp. 1-9, Dec. 2020.

[48] A. Maghawry, R. Hodhod, Y. Omar, and M. Kholief, "An approach for optimizing multi-objective problems using hybrid genetic algorithms," *Soft Computing*, vol. 25, pp. 389–405, Jan. 2021.

[49] H. T. Phong and P. Yenradee, "Vendor Managed Inventory for multi-vendor single manufacturer supply chain: A case study of instant noodle industry," *Engineering Journal*, vol. 24, no. 6, pp. 91-107, Nov. 2020.

[50] G. Gunawana, Y. Yanuarb, F. A. Waskitac and A. Kurniawan, "Modularization of ship engine room using Design Structure Matrix (DSM) based on the Genetic Algorithm," *Engineering Journal*, vol. 24, no. 4, pp. 206-216, July 2020.

[51] B. Singh, R. Kumar, and J. Singh Chohan, "Multi-objective optimization of 3D printing process using genetic algorithm for fabrication of copper reinforced ABS parts," *Materials Today: Proceedings*, pp. 1-8, Jun. 2021.

[52] I. M. Chew, F. Wong, J. Nandong, A. Bono, and K. I. Wong, "Three-element control system manipulation in steam generation for palm oil industry," *Advanced Science Letters*, vol. 23, no. 11, pp. 11475-11478, Nov. 2017.

[53] A. A. Motlagh, N. Shabakhty, and A. Kaveh, "Design optimization of jacket offshore platform considering fatigue damage using Genetic Algorithm," *Ocean Eng.*, vol. 227, no. 1, pp. 1-10, Mar. 2021.

[54] A. A. Muhammad Zahir, S. S. Nazli Alhady, and W.A. Wajdi Othman, "Objective functions modification of GA optimized PID controller for brushed DC motor," *Int. J. of Electrical and Computer Eng.,* vol. 10, no. 3, pp. 2426-2433, 2020.

[55] H. Tseng, P. Chu, H. Lu, and M. Tsai, "Easy particle swarm optimization for nonlinear constrained optimization problems," *IEEE Access*, vol. 9, pp. 124757-124767, Sept. 2021.

[56] L. K. Jang, "Feedback control for liquid level in a gravity-drained multi-tank system," *Chem. Eng. & Process Tech.*, vol. 3, no. 1, pp. 1-10, Jul. 2017.

Ing Ming Chew received the Bachelor of Engineering degree in electrical engineering (major in instrumentation and control) from the University Tun Hussein Onn, Batu Pahat, Johor, Malaysia, in 2002 and the Ph.D. degree in electrical and electronics engineering from University Malaysia Sabah, Sabah, Malaysia, in 2020. He is currently a lecturer at Curtin University Malaysia in Miri, Sarawak, Malaysia. Since 2020, he served as the program coordinator for the Bachelor of Electrical and Electronics Engineering, Electrical and Computer Department from Curtin University Malaysia. Dr. Chew has published more than 15 articles (for Journal and conference papers). In 2021, he received the Best Paper Awards for his latest paper submission to the International Conference in Green Energy, Computing and Sustainable Technology(GECOST-2021). His research interest includes Proportional-Integral-Derivative Control, Optimization analysis, and Internet of Things Embedded Systems.

Filbert H. Juwono received the B.Eng degree in electrical engineering and M.Eng degree in telecommunication engineering from the University of Indonesia, Depok, Indonesia in 2007 and 2009, respectively, and the Ph.D. degree in electrical and electronic engineering from The University of Western Australia, Perth, WA, Australia in 2017. He is currently a senior lecturer with the Department of Electrical and Computer Engineering, Curtin University Malaysia. His research interests include signal processing for communications, wireless communications, power-line communications, machine learning applications, and biomedical engineering. Dr. Juwono was a recipient of the prestigious Australian Awards Scholarship in 2012. Currently, he serves as an Associate Editor for IEEE Access, a Review Editor for Frontiers in Signal Processing, and an Editor-in-Chief for a newly established journal Green Intelligent Systems and Applications.

Wei Kitt Wong received the M.Eng. and Ph.D. degrees from Universiti Malaysia Sabah in 2012 and 2016, respectively in Computer Engineering. Prior to joining academia, he was with the telecommunication and building services industry. He is currently serving as a Senior Lecturer with the Department of Electrical and Computer Engineering, Curtin University Malaysia. His research interests include embedded system development, machine learning applications, and image processing.